IOPscience iopscience.iop.org

Home Search Collections Journals About Contact us My IOPscience

The effect of anisotropy on the ground-state magnetic ordering of the spin-1 quantum J_1^{XXZ}–J_2^{XXZ} model on the square lattice

This article has been downloaded from IOPscience. Please scroll down to see the full text article.

2008 J. Phys.: Condens. Matter 20 415213

(http://iopscience.iop.org/0953-8984/20/41/415213)

View the table of contents for this issue, or go to the journal homepage for more

Download details:
IP Address: 129.252.86.83
The article was downloaded on 29/05/2010 at 15:36

Please note that terms and conditions apply.

J. Phys.: Condens. Matter **20** (2008) 415213 (11pp) doi:10.1088/0953-8984/20/41/415213

The effect of anisotropy on the ground-state magnetic ordering of the spin-1 quantum J_1^{XXZ}–J_2^{XXZ} model on the square lattice

R F Bishop[1,2], P H Y Li[1,2], R Darradi[3], J Richter[3] and C E Campbell[2]

[1] School of Physics and Astronomy, Schuster Building, The University of Manchester, Manchester M13 9PL, UK
[2] School of Physics and Astronomy, University of Minnesota, 116 Church Street SE, Minneapolis, MN 55455, USA
[3] Institut für Theoretische Physik, Universität Magdeburg, 39016 Magdeburg, Germany

Received 28 May 2008, in final form 25 August 2008
Published 16 September 2008
Online at stacks.iop.org/JPhysCM/20/415213

Abstract

We study the zero-temperature phase diagram of the J_1^{XXZ}–J_2^{XXZ} Heisenberg model for spin-1 particles on an infinite square lattice interacting via nearest-neighbour ($J_1 \equiv 1$) and next-nearest-neighbour ($J_2 > 0$) bonds. The two bonds have the same XXZ-type anisotropy in spin space. The effects on the quasiclassical Néel-ordered and collinear stripe-ordered states of varying the anisotropy parameter Δ are investigated using the coupled cluster method carried out up to high orders. By contrast with the case for spin-$\frac{1}{2}$ particles studied previously, no intermediate disordered phase between the Néel and collinear stripe phases, for any value of the frustration J_2/J_1, for either the z-aligned ($\Delta > 1$) or xy-planar-aligned ($0 \leqslant \Delta < 1$) states, is predicted here. The quantum phase transition is determined as first order for all values of J_2/J_1 and Δ. The position of the phase boundary $J_2^c(\Delta)$ is determined accurately. It is observed to deviate most from its classical position $J_2^c = \frac{1}{2}$ (for all values of $\Delta > 0$) at the Heisenberg isotropic point ($\Delta = 1$), where $J_2^c(1) = 0.55 \pm 0.01$. By contrast, at the XY isotropic point ($\Delta = 0$), we find $J_2^c(0) = 0.50 \pm 0.01$. In the Ising limit ($\Delta \to \infty$), $J_2^c \to 0.5$ as expected.

(Some figures in this article are in colour only in the electronic version)

1. Introduction

In a recent paper [1] we have used the coupled cluster method (CCM) [2–4] to study the influence of spin anisotropy on the ground-state (gs) magnetic ordering of an anisotropic version (namely, the J_1^{XXZ}–J_2^{XXZ} model) of the well-known J_1–J_2 model on the infinite two-dimensional (2D) square lattice, described below, for particles with spin quantum number $s = \frac{1}{2}$. In the present paper we further the investigation of the J_1^{XXZ}–J_2^{XXZ} model by replacing the spin-$\frac{1}{2}$ particles by particles with $s = 1$.

The main purpose of the previous paper was to examine carefully the role of spin anisotropy in tuning the quantum fluctuations that play such a key role in determining the quantum phase diagram of the pure (spin-isotropic) J_1–J_2 model that has become an archetypal model for discussing the subtle interplay between the effects due to quantum fluctuations and frustration, as discussed below. While increasing the spin quantum number s is, of course, expected to reduce the effects of quantum fluctuations, new and unexpected phenomena may also arise. Thus, a well-known example of such new behaviour emerging when s is increased is the appearance of the gapped Haldane phase [5] in $s = 1$ one-dimensional (1D) chains, which is not present in their $s = \frac{1}{2}$ counterparts.

The basic (spin-isotropic) J_1–J_2 model with nearest-neighbour (NN) and next-nearest-neighbour (NNN) antiferromagnetic exchange interactions, of strengths J_1 and J_2

 © 2008 IOP Publishing Ltd Printed in the UK

respectively, has been extensively studied both theoretically [6–20] and experimentally [21–24]. Many of the earlier studies were motivated, at least in part, by the hope of shedding light on the possible link between antiferromagnetism and the onset of superconductivity at high temperature in the doped cuprate materials whose undoped precursors are seemingly well described by the $s = \frac{1}{2}$ version of the J_1–J_2 model on the square lattice in two dimensions [8, 25–27]. The recent discovery of several other quasi-2D materials that are realizations of the J_1–J_2 model, has only served to extend the theoretical interest in the model.

Some of the actual magnetic compounds that can be well described by the $s = \frac{1}{2}$ J_1–J_2 model are La_2CuO_4 [27] for small values of J_2/J_1, and Li_2VOSiO_4 and Li_2VOGeO_4 [21, 22] for large values of J_2/J_1. Other such materials include the compounds $VOMoO_4$ [23] and $Pb_2VO(PO_4)_2$ [24]. The compound $VOMoO_4$ is interesting because its exchange couplings appear to be more than an order of magnitude larger than those of Li_2VOSiO_4, even though the structures of the two compounds are closely related. Similarly, the compound $Pb_2VO(PO_4)_2$ also has a structure closely related to that of Li_2VOSiO_4, but it appears to have a ferromagnetic NN exchange coupling ($J_1 < 0$) frustrated by an antiferromagnetic NNN exchange coupling ($J_2 > 0$), with $|J_2/J_1| \approx 1.5$. By contrast, although all of the other compounds mentioned above are also examples of quasi-2D frustrated spin-$\frac{1}{2}$ magnets, they have NN and NNN exchanges that are both antiferromagnetic.

For the past few decades, a great deal of attention has also been devoted to magnetic materials with spin-1 ions, such as the linear chain systems including $CsNiCl_3$ [28] with a weak axial anisotropy, $CsFeBr_3$ [29] with a strong planar anisotropy and the complex materials NENP ($Ni(C_2H_8N_2)_2NO_2(ClO_4)$) [30] with a weak planar anisotropy and NENC ($Ni(C_2H_8N_2)_2Ni(CN_4)$) [31] with a strong planar anisotropy; as well as the 2D Heisenberg antiferromagnet K_2NiF_4 [32]. The spin gaps observed in $CsNiCl_3$ and NENP are believed to be examples of the integer-spin gap behaviour predicted by Haldane [5]; whereas half-odd-integer spin systems are gapless. Another new spin-gapped material is the 2D triangular lattice antiferromagnet $NiGa_2S_4$ [33] which, it has been argued [34, 35], may be a 'spin nematic' [36]. It is clear, therefore, that the theoretical study of 2D spin-1 quantum magnets is worthy of pursuit.

In this context we note the recent discovery of superconductivity with a transition temperature at $T_c \approx 26$ K in the layered iron-based compound LaOFeAs, when doped by partial substitution of the oxygen atoms by fluorine atoms [37], $La[O_{1-x}F_x]FeAs$, with $x \approx 0.05$–0.11. This has been followed by the rapid discovery of superconductivity at even higher values of T_c ($\gtrsim 50$ K) in a broad class of similar doped quaternary oxypnictide compounds. Enormous interest has thereby been engendered in this class of materials. Of particular relevance to the present work are the very recent first-principles calculations [38] showing that the undoped parent precursor material LaOFeAs is well described by the spin-1 J_1–J_2 model on the square lattice with $J_1 > 0$, $J_2 > 0$, and $J_2/J_1 \approx 2$. Broadly similar conclusions have also been reached by other authors [39].

Many of the above quasi-2D magnetic materials, and many others like them, display interesting gs phases, often with subtle quantum phase transitions between them. Generically, the interplay between reduced dimensionality, competing interactions and strong quantum fluctuations, seems to generate a number of new states of condensed matter with orderings that differ from the usual states of quasiclassical long-range order (LRO). Thus, for high-temperature superconductivity, for example, Anderson [25] has suggested that quantum spin fluctuations and frustration due to doping could lead to the collapse of the 2D Néel-ordered antiferromagnetic phase present at zero doping, and that this could be a mechanism that drives the superconducting behaviour. This, and many similar experimental observations for other magnetic materials of reduced dimensionality, has intensified the study of order–disorder quantum phase transitions. Thus, low-dimensional quantum antiferromagnets have attracted much recent attention as model systems in which strong quantum fluctuations might be able to destroy magnetic LRO in the ground state (GS). In the present paper we consider a system of $N \to \infty$ spin-1 particles on a spatially isotropic 2D square lattice.

The isotropic Heisenberg antiferromagnet with only nearest-neighbour (NN) bonds, all of equal strength ($J_1 > 0$), exhibits magnetic LRO at zero temperature on such bipartite lattices as the square lattice considered here. A key mechanism that can then serve to destroy the LRO for such systems (with a given lattice and spins of a given spin quantum number s) is the introduction of competing or frustrating bonds on top of the NN bonds. The interested reader is referred to [40, 41] for a more detailed discussion of 2D spin systems in general.

In this context, and as we have already noted above, an archetypal frustrated model of the above type that has attracted much theoretical attention in recent years is the 2D J_1–J_2 model on a square lattice with both NN and NNN antiferromagnetic interactions, with strength $J_1 > 0$ and $J_2 > 0$ respectively. The NN bonds $J_1 > 0$ promote Néel antiferromagnetic order, while the NNN bonds $J_2 > 0$ act to frustrate or compete with this order. All such frustrated quantum magnets continue to be of great theoretical interest because of the possible spin-liquid and other such novel magnetically-disordered phases that they can exhibit (and see, e.g., [42–44]).

The properties of the $s = 1/2$ J_1–J_2 model on the 2D square lattice are well understood in the limits when $J_2 = 0$ or $J_1 = 0$. For the case when $J_2 = 0$, and the classical GS is perfectly Néel-ordered, the quantum fluctuations are not sufficiently strong enough to destroy the Néel LRO, although the staggered magnetization is reduced to about 61% of its classical value. The opposite limit of large J_2 is a classic example [8] of the phenomenon of order by disorder [45, 46]. Thus, in the case where $J_1 \to 0$ with $J_2 \neq 0$ and fixed, the two sublattices each order antiferromagnetically at the classical level, but in directions which are independent of each other. This degeneracy is lifted by quantum fluctuations and the GS becomes magnetically ordered collinearly as a stripe phase consisting of successive alternating rows (or columns) of parallel spins. It is by now also widely accepted that the

$s = 1/2$ J_1–J_2 model exhibits the above two quasiclassical antiferromagnetic phases with LRO at small and at large J_2 separated by an intermediate quantum paramagnetic phase without magnetic LRO in the parameter region $J_2^{c_1} < J_2 < J_2^{c_2}$ where $J_2^{c_1} \approx 0.4J_1$ and $J_2^{c_2} \approx 0.6J_1$. The GS at low $J_2 < J_2^{c_1}$ exhibits Néel-ordered magnetic LRO (with a wavevector $Q = (\pi, \pi)$), whereas the GS at large $J_2 > J_2^{c_2}$ exhibits collinear stripe-ordered magnetic LRO (with a wavevector $Q = (\pi, 0)$ or $Q = (0, \pi)$).

Given the key role played by quantum fluctuations in determining the gs structure of frustrated magnets, it is clearly of central interest to focus special attention on the various means by which we may vary or 'tune' them. Clearly, as we have already noted, an increase in the spin quantum number s is expected to decrease their strength. Thus, for example, for the simple case of the isotropic Heisenberg model on the square lattice with NN bonds all of the same strength, whereas the quantum fluctuations reduce the perfect Néel ordering in the classical case (i.e., $s \to \infty$) so that the staggered magnetization is only about 61% of its classical value for the $s = \frac{1}{2}$ case as noted above, the corresponding reduction in the $s = 1$ case is less, namely to about 80% of the classical value (and see [47] and references cited therein). One of the goals of the present paper is to investigate similarly the effect of increasing s for the archetypal J_1–J_2 model on the 2D square lattice. In order to do so it is convenient to consider at the same time any other means to 'tune' the quantum fluctuations. In particular, we note that besides changing s or the dimensionality and lattice type of the system, and apart from varying the relative strengths of the competing exchange interactions, another key mechanism to tune the quantum fluctuations is the introduction of anisotropy, either in real space [48–53] or in spin space [54–57], into the existing exchange bonds.

Turning first to the case of anisotropy in real (crystal lattice) space, we note that Nersesyan and Tsvelik [48] have recently introduced and studied an interesting generalization of the pure J_1–J_2 model for the $s = \frac{1}{2}$ case in order to investigate the effects of spatial anisotropy on the quantum fluctuations in the model. This extended model, the so-called J_1–J_1'–J_2 model, has been further studied by other groups for both the $s = \frac{1}{2}$ [49–52] and the $s = 1$ [53] cases. This generalization of the 2D J_1–J_2 model introduces a spatial anisotropy on the square lattice by allowing the NN bonds to have different strengths J_1 and J_1' in the two orthogonal spatial lattice dimensions, while keeping all of the NNN bonds across the diagonals to have the same strength J_2. In previous work of our own [52, 53] on this J_1–J_1'–J_2 model we studied the effect of the coupling J_1' on the semiclassical Néel-ordered and stripe-ordered phases. For the $s = \frac{1}{2}$ case, we found that the quantum critical points for both of these phases with LRO increase as the coupling ratio J_1'/J_1 is increased, and an intermediate phase with no magnetic LRO only emerges when $J_1'/J_1 \gtrsim 0.6$, with strong indications of a quantum triple point at $J_1'/J_1 \approx 0.60$, $J_2/J_1 \approx 0.33$. For $J_1'/J_1 = 1$, the results agree with the previously known results of the J_1–J_2 model described above.

By contrast, for the $s = 1$ case, we found no evidence for an intermediate phase between the Néel and stripe states, as compared with all previous results for the corresponding $s = \frac{1}{2}$ case. However, for the $s = 1$ case we found instead strong evidence for a quantum tricritical point at $J_1'/J_1 \approx 0.66$, $J_2/J_1 \approx 0.35$, where a line of second-order phase transitions between the quasiclassical Néel-ordered and stripe-ordered phases (for $J_1'/J_1 \lesssim 0.66$) meets a line of first-order phase transitions between the same two states (for $J_1'/J_1 \gtrsim 0.66$). For $J_1'/J_1 = 1$ the results obviously reproduce those of the usual spin-1 J_1–J_2 model, for which $J_2^c/J_1 \approx 0.55 \pm 0.01$.

Finally, we turn to the main subject of interest in this paper, namely to further the study of the 2D spin-1 J_1–J_2 model on the square lattice by introducing anisotropy in spin space. While the influence of the spin anisotropy on the $s = \frac{1}{2}$ J_1–J_2 model on the square lattice has been studied by various groups [54–57], including ourselves [1], relatively little is known for the $s = 1$ case.

Our aim here is to further the study of the J_1^{XXZ}–J_2^{XXZ} model for the $s = 1$ case, by making use of the coupled cluster method (CCM) carried out to high orders by making use of supercomputing resources. The CCM (see [2–4] and references cited therein) is one of the most powerful and most universally applicable of all known *ab initio* techniques of modern microscopic quantum many-body theory. It is also one of the most accurate methods available at attainable levels of computational implementation. We note, in the present context, that the CCM is a particularly effective tool for studying highly frustrated quantum magnets, where such other numerical methods as the quantum Monte Carlo method and the exact diagonalization method are often severely limited in practice, e.g., by the 'minus-sign problem' for the former case, and the very small sizes of the spin systems that can be handled in practice with available computing resources for the latter. This is especially true for spin systems with spin quantum number $s > \frac{1}{2}$, as are of interest here. The CCM has been applied successfully on many previous occasions to calculate the ground-state and excited-state properties of a diverse array of quantum spin systems [1, 4, 12, 47, 52, 53, 57–71].

2. The model

Exactly as for the $s = \frac{1}{2}$ case that we studied earlier [1], the $s = 1$ J_1–J_2 Heisenberg model employed here has two kinds of exchange bonds, namely the NN J_1 bonds along both the row and the column directions of the square lattice, and the NNN J_2 bonds along the diagonals of the squares. The model is then generalized by including an anisotropy in spin space in both types of bonds. The anisotropy parameter Δ is assumed to be the same in both exchange terms, thus producing the so-called J_1^{XXZ}–J_2^{XXZ} model, with a Hamiltonian given by

$$H = J_1 \sum_{\langle i,j \rangle} (s_i^x s_j^x + s_i^y s_j^y + \Delta s_i^z s_j^z) + J_2 \sum_{\langle\langle i,k \rangle\rangle} (s_i^x s_k^x + s_i^y s_k^y + \Delta s_i^z s_k^z), \quad (1)$$

where the sums over $\langle i, j \rangle$ and $\langle\langle i, k \rangle\rangle$ run over all NN and NNN pairs respectively, counting each bond once and once only. Both exchange couplings are assumed to be antiferromagnetic here (i.e., $J_1 > 0$ and $J_2 > 0$), and

henceforth the energy scale is set by putting $J_1 = 1$. We shall also only be concerned here with the case $\Delta \geqslant 0$.

The model has two types of classical ground state (GS), namely a z-aligned state for $\Delta > 1$ and an xy-planar-aligned state for $0 < \Delta < 1$. Since all directions in the xy-plane in spin space are equivalent, we may choose the direction arbitrarily for the xy-planar-aligned state to be the x-direction, say. Both of these z-aligned and x-aligned ground states further divide into a Néel (π, π) state and collinear stripe states (columnar stripe $(\pi, 0)$ and row stripe $(0, \pi)$). There is clearly a symmetry under the interchange of rows and columns, and hence we only consider the columnar stripe state. The Néel states are the classical GS for $J_2 < \frac{1}{2}J_1$, and the collinear stripe states are the classical GS for $J_2 > \frac{1}{2}J_1$. The (first-order) classical phase transition between these states of perfect classical LRO occurs precisely at $J_2^c = \frac{1}{2}J_1$.

3. The coupled cluster method

We now briefly describe the CCM formalism. For further details interested readers are referred, for example, to [2–4] and references cited therein.

In order to use the CCM the first step is always the choice of a normalized model (or reference) state $|\Phi\rangle$ which is required to act as a cyclic vector (or, more physically, as a generalized vacuum state) with respect to a complete set of mutually commuting multi-configurational creation operators, $C_I^+ \equiv (C_I^-)^\dagger$ that need to be chosen simultaneously. The index I here is a set-index that gives a complete labelling of the many-particle configuration created in the state $C_I^+|\Phi\rangle$. The requirements on $\{|\Phi\rangle; C_I^+\}$ are that any many-particle state can be exactly decomposed as a unique linear combination of the states $\{C_I^+|\Phi\rangle\}$, together with the conditions,

$$\langle\Phi|C_I^+ = 0 = C_I^-|\Phi\rangle \quad \forall I \neq 0; \qquad C_0^+ \equiv 1, \tag{2}$$

$$[C_I^+, C_J^+] = 0 = [C_I^-, C_J^-]. \tag{3}$$

The exact many-body gs ket and bra states, whose solutions we seek via the CCM calculation at hand, satisfy the respective Schrödinger equations,

$$H|\Psi\rangle = E|\Psi\rangle, \tag{4a}$$

$$\langle\tilde{\Psi}|H = E\langle\tilde{\Psi}|, \tag{4b}$$

respectively, with the normalization defined by $\langle\tilde{\Psi}|\Psi\rangle = 1$ (i.e., with $\langle\tilde{\Psi}| = (\langle\Psi|\Psi\rangle)^{-1}\langle\Psi|$), and with $|\Psi\rangle$ itself satisfying the intermediate normalization condition $\langle\Phi|\Psi\rangle = 1 = \langle\Phi|\Phi\rangle$. In terms of the set $\{|\Phi\rangle; C_I^+\}$, the CCM now employs an exponential parametrization for the exact gs ket energy eigenstate,

$$|\Psi\rangle = \mathrm{e}^S|\Phi\rangle, \qquad S = \sum_{I\neq 0} \mathcal{S}_I C_I^+, \tag{5a}$$

that lies at the heart of the method. Its counterpart for the exact gs bra energy eigenstate is chosen as

$$\langle\tilde{\Psi}| = \langle\Phi|\tilde{S}\mathrm{e}^{-S}, \qquad \tilde{S} = 1 + \sum_{I\neq 0} \tilde{\mathcal{S}}_I C_I^-. \tag{5b}$$

The gs CCM correlation operators, S and $\tilde{S}$, contain the real c-number correlation coefficients, $\mathcal{S}_I$ and $\tilde{\mathcal{S}}_I$, that need to be calculated. Clearly, once they are known, all other gs properties of the many-body system can be derived from them. In order to find them we simply insert the parametrizations (5*a*) and (5*b*) into the Schrödinger equations (4*a*) and (4*b*), and then project onto the complete sets of states $\langle\Phi|C_I^-$ and $C_I^+|\Phi\rangle$, respectively. Completely equivalently, we may simply demand that the gs energy expectation value, $\bar{H} \equiv \langle\tilde{\Psi}|H|\Psi\rangle$, is minimized with respect to the entire set $\{\mathcal{S}_I, \tilde{\mathcal{S}}_I\}$. In either case we are easily led to the equations

$$\langle\Phi|C_I^-\mathrm{e}^{-S}H\mathrm{e}^S|\Phi\rangle = 0; \qquad \forall I \neq 0, \tag{6a}$$

$$\langle\Phi|\tilde{S}\mathrm{e}^{-S}[H, C_I^+]\mathrm{e}^S|\Phi\rangle = 0; \qquad \forall I \neq 0, \tag{6b}$$

which are first derived using computer algebra and then solved for the set $\{\mathcal{S}_I, \tilde{\mathcal{S}}_I\}$ within specific truncation schemes described below, by making use of parallel computing routines [72]. Equation (6*a*) also shows that the gs energy at the stationary point has the simple form

$$E = E(\{\mathcal{S}_I\}) = \langle\Phi|\mathrm{e}^{-S}H\mathrm{e}^S|\Phi\rangle. \tag{7}$$

It is important to realize that this bi-variational formulation does not necessarily lead to an upper bound for E when the summations for S and $\tilde{S}$ in (5*a*) and (5*b*) are truncated, due to the lack of manifest Hermiticity when such approximations are made. Nonetheless, one can prove [3] that the important Hellmann–Feynman theorem *is* preserved in all such approximations.

Equation (6*a*) represents a coupled set of nonlinear multinomial equations for the c-number correlation coefficients $\{\mathcal{S}_I\}$. The nested commutator expansion of the similarity-transformed Hamiltonian,

$$\mathrm{e}^{-S}H\mathrm{e}^S = H + [H, S] + \frac{1}{2!}[[H, S], S] + \cdots, \tag{8}$$

and the fact that all of the individual components of S in the expansion of (5*a*) commute with one another by construction, as in (3), together imply that each element of S in (5*a*) is linked directly to the Hamiltonian in each of the terms in (8). Each of the coupled equations (6*a*) is hence of Goldstone *linked-cluster* type, which thereby guarantees that all extensive variables, such as the energy, scale linearly with particle number, N. Thus, at any level of approximation obtained by truncation in the summations on the index I in (5*a*) and (5*b*), we may always work safely from the outset in the limit $N \to \infty$ of an infinite system, as we do in all our calculations below. It is also important to note that each of the linked-cluster equations (6*a*) is actually of finite length when expanded, since the otherwise infinite series of (8) will always terminate at a finite order, provided only that each term in the Hamiltonian, H, contains a finite number of single-particle destruction operators defined with respect to the reference (vacuum) state $|\Phi\rangle$, as in the case of our Hamiltonian (1).

We turn now to the implementation of the CCM for quantum spin systems, for which it is usually convenient to take the classical ground states as our (initial) choices for the

model state $|\Phi\rangle$. Hence, we may choose here either a Néel state or a collinear (columnar) stripe state for $|\Phi\rangle$. Each of these can be further sub-divided into a z-aligned choice or an xy-planar (say, x-aligned) choice, which we expect to be appropriate for the regions $\Delta \geqslant 1$ and $0 \leqslant \Delta \leqslant 1$ respectively on purely classical grounds. We present results in section 4 based on all four of these classical ground states as choices for $|\Phi\rangle$. In order to implement the CCM computationally it is very convenient to treat the spins on every lattice site in any chosen model state $|\Phi\rangle$ as equivalent. In order to do so we introduce a different local quantization axis and a correspondingly different set of spin coordinates on each site, so that all spins, whatever their original orientations in $|\Phi\rangle$ in the global spin-coordinate system, align along the negative z-direction, say, in these local spin coordinates. This can always be done by defining a suitable rotation in spin space of the global spin coordinates at each lattice site. Such rotations are canonical transformations that leave the spin commutation relations unchanged. In these local spin axes where the configuration indices I simply become a set of lattice site indices, $I \rightarrow \{k_1, k_2, \ldots, k_m\}$, the generalized multi-configurational creation operators C_I^+ are simple products of single spin-raising operators, $C_I^+ \rightarrow s_{k_1}^+ s_{k_2}^+ \cdots s_{k_m}^+$, where $s_k^\pm \equiv s_k^x \pm \mathrm{i} s_k^y$, and (s_k^x, s_k^y, s_k^z) are the usual $SU(2)$ spin operators on lattice site k. For the quasiclassical magnetically-ordered states that we calculate here, the order parameter is the sublattice magnetization, M, which is given within our local spin coordinates defined above as

$$M \equiv -\frac{1}{N}\langle\tilde{\Psi}|\sum_{k=1}^{N} s_k^z|\Psi\rangle. \tag{9}$$

The CCM formalism is clearly exact if one includes all spin configurations I in the expansions (5*a*) and (5*b*) of the S and $\tilde{S}$ operators respectively. However, truncations are necessary in practice. Based on a great deal of previous experience, we usually employ the so-called LSUBn approximation scheme for $s = 1/2$ quantum spin systems (see [52] and references cited therein), and its so-called SUBn–m counterpart for $s = 1$ systems (see [53] and references cited therein). The LSUBn scheme is defined such that all possible multi-spin-flip correlations over different locales on the lattice defined by n or fewer contiguous lattice sites are retained at the nth level of approximation. For the case of spins with $s = \frac{1}{2}$, the multi-configurational creation operators, C_I^+ can contain no more than one spin-raising operator s_j^+ for each lattice site j. However, the number of fundamental LSUBn configurations for $s = 1$ becomes appreciably higher than for $s = \frac{1}{2}$, since each spin on each site j can now be flipped twice by the spin-raising operators, so that in this case the multi-configurational creation operators, C_I^+ can contain up to two spin-raising operator s_j^+ for each lattice site j. Thus, for systems with $s > \frac{1}{2}$ it is more practical to use the SUBn–m scheme, in which all correlations involving no more than n spin-flips spanning a range of no more than m adjacent lattice sites are retained. Clearly, for spins with $s = 1$, the SUB2n–n scheme is fully equivalent to the LSUBn scheme. More generally for spins with arbitrary spin quantum number s, SUB2sn–n $\equiv$ LSUBn. In order to keep the number of fundamental configurations from growing too quickly with increasing level of approximation we set $m = n$, and thus we have the SUBn–n scheme. The approximation clearly becomes exact as $n \rightarrow \infty$.

Table 1. Numbers of fundamental configurations (♯ f.c.) retained in the CCM SUBn–n approximation for the z-aligned states and the planar x-aligned states of the $s = 1$ J_1^{XXZ}–J_2^{XXZ} model on the square lattice.

	z-aligned states		Planar x-aligned states	
	♯ f.c.		♯ f.c.	
Scheme	Néel	Stripe	Néel	Stripe
SUB2–2	1	1	2	3
SUB4–4	15	21	31	57
SUB6–6	375	585	1085	2131
SUB8–8	17 864	29 411	61 904	12 3471

We note that, in general terms, both the LSUBn and SUBn–m truncation schemes are systematic *localized* approximation hierarchies in which the truncation indices are physically related to the size of the clusters of spins on the lattice for which the multi-spin correlations are explicitly included. Their physical motivation (and eventual justification) thus stems ultimately from the localized short-range nature of the underlying Hamiltonian (which, in the present case, involves just two-spin interactions at NN and NNN distances apart only). The maximum number of spins correlated in such clusters is n in both cases. By contrast, the SUBn scheme (which is formally equivalent to the SUBn–m scheme in the limit $m \rightarrow \infty$) explicitly correlates all clusters of spins involving no more than n spin-flips, regardless of the spatial separations of the spins within the correlated clusters. It is important to note however that in *all* CCM approximations (including the LSUBn and SUBn–m schemes) each correlated cluster configuration retained within the correlation operator S of (5*a*) is actually counted an *arbitrarily large* number of times due to the exponentiated form in which the operator S appears in the parametrization (5*a*). It is precisely the exponential form that guarantees the proper counting of arbitrary multiples, at different positions on the lattice, of each configuration (and all products of such multiples for different configurations) retained in S, considered as *independent* excitations. Thus, even though, for example, the LSUBn and SUBn–m truncation schemes are motivated by the inclusion of the explicit correlations within localized clusters of spins only up to a given size, every approximation includes configurations in which an *arbitrary* number of spins (up to all $N \rightarrow \infty$ spins) are correlated, albeit as (properly counted) products of independent sub-clusters up to a given finite size.

Table 1 shows the number of fundamental SUBn–n configurations for the z-aligned and planar x-aligned states in the Néel and striped phases. We see that the number of fundamental configurations for the planar model state at the SUB8–8 level of approximation is 61904 for the Néel phase and 123471 for the stripe phase. The intensive calculations required at even this very high order of approximation are easily practicable with relatively modest supercomputing resources. Thus, for example, we employed 200 processors

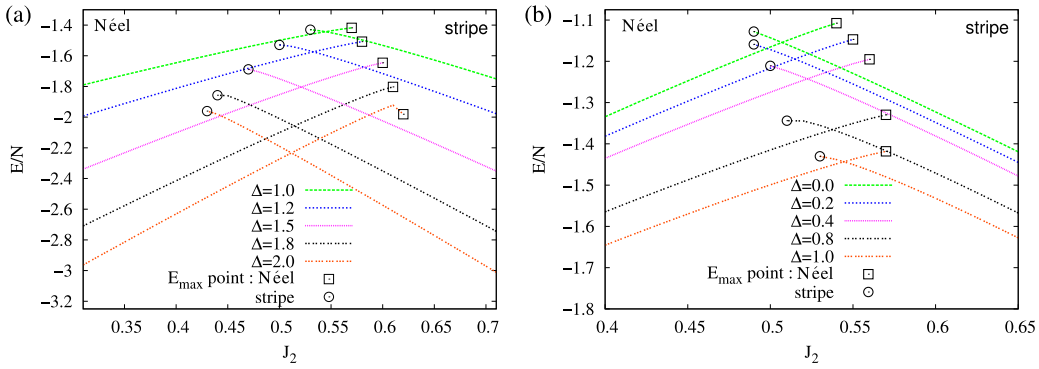

Figure 1. Extrapolated CCM SUBn–n results using the z-aligned (a) and planar x-aligned (b) states for the gs energy, E/N, for the Néel and stripe phases of the $s = 1$ J_1^{XXZ}–J_2^{XXZ} model. The SUBn–n results are extrapolated to the limit $n \to \infty$ using the sets $n = \{2, 4, 6, 8\}$ for both the z-aligned and planar x-aligned states. The NN exchange coupling $J_1 = 1$. The meaning of the $E_{\max}$ points shown is described in the text.

simultaneously to execute the SUB8–8 calculations using the planar x-aligned collinear stripe state as model state, and with this number of processors it took about 6 h to solve the CCM equations (6*a*) and (6*b*) at this level of approximation for each value of the anisotropy parameter Δ in the Hamiltonian (1).

Clearly, the last step in our calculations is to extrapolate the approximate SUBn–n results to the exact, $n \to \infty$, limit. We use here for the extrapolations of the raw SUBn–n data the same well-tested scaling laws as we used previously in our studies of the J_1–J_1'–J_2 model for both the $s = \frac{1}{2}$ case [52] and the $s = 1$ case [53], as well as for the $s = \frac{1}{2}$ version of the present model [1]. Thus, the scaling law used for the gs energy per spin, E/N, is

$$E/N = a_0 + a_1 n^{-2} + a_2 n^{-4}, \tag{10}$$

and that for the staggered magnetization, M, is

$$M = b_0 + n^{-0.5}\left(b_1 + b_2 n^{-1}\right). \tag{11}$$

In order to have a robust and stable fit to any fitting formula that contains m unknown parameters, it is well known that it is desirable to have at least $(m + 1)$ data points (the so-called $m + 1$ rule). Both of our scaling laws (10) and (11) contain $m = 3$ unknown parameters to be determined, and in all cases we have SUBn–n data sets with $n = \{2, 4, 6, 8\}$. In all our results presented below the SUBn–n results are extrapolated to the limit $n \to \infty$ using the sets with $n = \{2, 4, 6, 8\}$ for both the z-aligned and planar x-aligned states. However, we have also extrapolated E/N and M using the sets $n = \{4, 6, 8\}$ and $n = \{2, 4, 6\}$. In all cases they lead to very similar results, thereby adding credence to their validity and stability. We also note that for the corresponding $s = 1/2$ model we could perform LSUBn $\equiv$ SUBn–n approximation calculations for $n = \{2, 4, 6, 8, 10\}$. This enabled us to perform extrapolations using the sets $n = \{2, 4, 6, 8\}$ and $n = \{2, 4, 6, 8, 10\}$ as well as the preferred set $n = \{4, 6, 8, 10\}$. Gratifyingly, all sets yielded very similar extrapolated results, even near phase boundaries and the quantum triple point, which gives us great confidence in the accuracy and robustness of our extrapolation scheme.

4. Results

Figure 1 shows the extrapolated CCM results for the gs energy per spin, E/N, as a function of J_2 for various values of Δ, using both the z-aligned and planar x-aligned model states. For each value of Δ two curves are shown, one (for smaller values of J_2) using the Néel state, and the other (for larger values of J_2) using the stripe state as CCM model state. As has been discussed in detail elsewhere [3, 4, 63], the coupled sets of LSUBn equations (6*a*) have natural termination points (at least for values $n > 2$) for some critical value of a control parameter (here the anisotropy, Δ), beyond which no real solutions to the equations exist. Thus, for each set of calculations based on one of the four CCM model states used, the $E_{\max}$ points shown in figure 1 are either those natural termination points described above for the highest (SUB8–8) level of approximation we have implemented, or the points where the gs energy becomes a maximum should the latter occur first (i.e., as one approaches the termination point). The advantage of this usage of the $E_{\max}$ points is that we do not then display gs energy data in any appreciable regimes where SUBn–n calculations with very large values of n (higher than can feasibly be implemented) would not have solutions, because of having terminated already.

All of the curves such as those shown in figure 1 illustrate very clearly that the corresponding pairs of gs energy curves (for the same values of Δ) for the Néel and stripe phases cross one another, for both the z-aligned (figure 1(a) for all values $\Delta > 1$) and the x-aligned (figure 1(b) for all values $0 \leqslant \Delta < 1$) cases. The crossings occur with a clear discontinuity in slope, which is completely characteristic of a first-order phase transition, exactly as observed in the classical (i.e., $s \to \infty$) case. Unlike in the $s = \frac{1}{2}$ version of this model that we studied earlier [1], there is no indication at all in the present $s = 1$ case of any intermediate paramagnetic phase emerging for any values of the parameters J_2 and Δ. Furthermore, the direct first-order phase transition, so indicated by our results for the gs energy, between the quasiclassical Néel-ordered and collinear stripe-ordered phases, in both the z-aligned and planar x-aligned cases, occurs for all values of $\Delta \geqslant 0$ very close to the classical

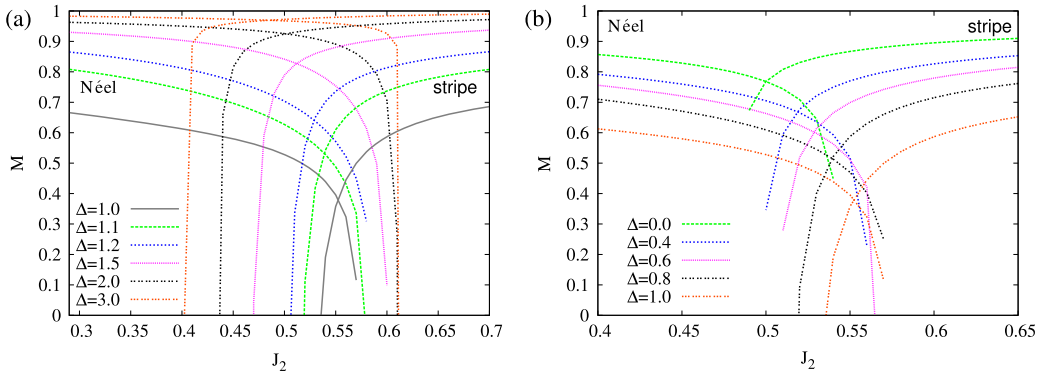

Figure 2. Extrapolated CCM SUBn–n results using the z-aligned (a) and planar x-aligned (b) states for the gs staggered magnetization, M, for the Néel and stripe phases of the $s = 1$ J_1^{XXZ}–J_2^{XXZ} model. The SUBn–n results are extrapolated to the limit $n \to \infty$ using the sets $n = \{2, 4, 6, 8\}$ for both the z-aligned state and the planar x-aligned states. The NN exchange coupling $J_1 = 1$.

phase boundary $J_2^c = \frac{1}{2}$, the point of maximum (classical) frustration.

We show in figure 2 corresponding indicative sets of CCM results, based on the same four model states, for the gs order parameter (namely, the staggered magnetization), to those shown in figure 1 for the gs energy. The staggered magnetization data completely reinforce the phase structure of the model as deduced above from the gs energy data.

Thus, let us now denote by M_c the quantum phase transition point deduced from curves such as those shown in figure 2, where M_c is generically defined to be either (a) the point where corresponding pairs of CCM staggered magnetization curves (for the same value of Δ), based on the Néel and stripe model states, intersect one another if they do so at a physical value $M \geqslant 0$; or (b) if they do not so intersect at a value $M \geqslant 0$, the two points where the corresponding values of the staggered magnetization go to zero. Clearly, in this generic scenario, case (a) corresponds to a direct phase transition between the Néel and stripe phases, which will generally be first order if the intersection point has a value $M \neq 0$ (and, only exceptionally, second order, if the crossing occurs exactly at $M = 0$). On the other hand, case (b) corresponds to the situation where the points where the LRO vanishes for both quasiclassical (i.e., Néel-ordered and stripe-ordered) phases are indicative of a phase transition from each of these phases to some intermediate magnetically-disordered phase. A detailed discussion of this order parameter criterion for a phase transition and its relation to the stricter energy crossing criterion has been given elsewhere [69].

It is clear from figures 2(a) and (b) that case (b) above never occurs for the present spin-1 model for any values of the anisotropy parameter Δ or for any values of the NNN exchange coupling J_2, unlike in the $s = \frac{1}{2}$ version of this model that we studied earlier [1].

By putting together data of the sort shown in figures 1 and 2 we can now deduce the gs phase diagram of our system from our CCM calculations based on the four model states with quasiclassical antiferromagnetic LRO that we have employed. Figure 3 shows the zero-temperature gs phase diagram of the 2D $s = 1$ J_1^{XXZ}–J_2^{XXZ} model on the square lattice for the z-aligned and planar x-aligned states, as obtained from

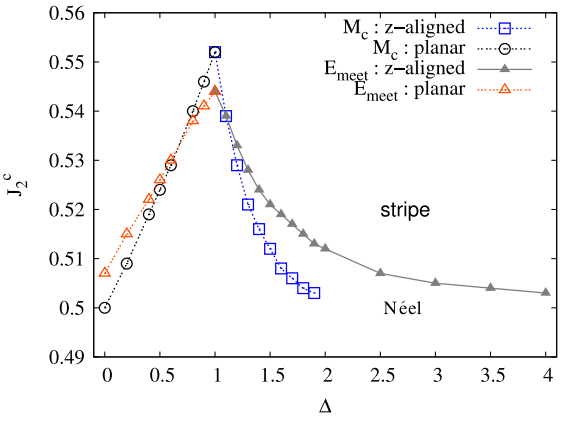

Figure 3. Extrapolated CCM SUBn–n results using the z-aligned and planar x-aligned states for the ground-state phase diagram of the $s = 1$ J_1^{XXZ}–J_2^{XXZ} anisotropic Heisenberg model on the square lattice, for the NN exchange coupling $J_1 = 1$. The SUBn–n results for the energy per spin and the staggered magnetization are extrapolated to the limit $n \to \infty$ using the sets $n = \{2, 4, 6, 8\}$ for both the z-aligned and planar x-aligned model states. $M_c \equiv$ magnetization critical point, defined in the text. E_{meet} denotes the crossing point of the CCM energy curves for the same value of Δ based on the Néel-ordered and collinear stripe-ordered model states.

our extrapolated results for both the gs energy and the gs order parameter. The completely independent results from both the energy criterion and the order parameter criterion for the phase transition give extremely similar positions for the phase boundary, as one can observe from figure 3. Note that the results from using the order parameter criterion become increasingly inaccurate for large values of Δ, and this is why we show them in figure 3 only out to $\Delta \lesssim 2$. The reason for this is simple. Thus, as $\Delta \to \infty$, the order parameters $M \to 1$ for both the Néel-ordered and collinear stripe-ordered phases, and it becomes increasingly difficult to determine the point where they cross, since the angle of their crossing becomes vanishingly small. This effect can clearly be seen in figure 2(a), where it has clearly become acute even for values of Δ as small as about 2. On the other hand, the energy criterion correspondingly becomes *more* accurate as $\Delta \to \infty$, as one may observe from figure 1(a). Thus, figure 3 clearly shows

that the phase boundary approaches the classical line $J_2^c = 0.5$ as $\Delta \to \infty$, as expected in this Ising-like limit.

Our results certainly provide very clear and consistent evidence that there exists no intermediate phase. Thus, the curves for the order parameters of the Néel and stripe phases always meet at a finite value and the corresponding curves for the gs energies of the two phases intersect with a discontinuity in slope, for both the z-aligned and planar x-aligned states, for all values of the anisotropy parameter Δ. All of the evidence clearly points towards a first-order phase transition between the two phases.

We note also that the z-aligned and xy-planar-aligned phases meet precisely at the isotropic point $\Delta = 1$, just as in the classical case, and exactly as expected. However, this does provide a consistency check on our independent numerical calculations for the two phases. The case $\Delta = 1$ obviously reproduces the usual (isotropic) J_1–J_2 model. Thus, at $\Delta = 1$, we find $J_2^c = 0.55 \pm 0.01$ which, very encouragingly, is the same value we found [53] for the $s = 1$ J_1–J_1'–J_2 model in the spatially isotropic limiting case when $J_1'/J_1 = 1$. We also note that in the present spin-1 quantum model, the isotropic point $\Delta = 1$ is precisely the point at which the boundary between the two quasiclassical phases deviates most from its classical position at $J_2^c = \frac{1}{2}$ for all values of $\Delta \geqslant 0$. Our calculations also indicate that at the isotropic XY point of the model (i.e., where $\Delta = 0$) the phase boundary is at $J_2^c = 0.50 \pm 0.01$.

5. Discussion

Our results have clearly shown in detail how the quantum fluctuations present in the spin-1 J_1–J_2 model on the infinite square lattice are diminished by varying the spin anisotropy parameter Δ away from the Heisenberg isotropic point $\Delta = 1$ in either direction. This is precisely as was observed previously [1] for the spin-$\frac{1}{2}$ version of the same model, and as was to be expected. However, unlike what would be predicted by lowest-order (or linear) spin-wave theory (LSWT) [6], for example, we can now conclude with confidence from our results that no such intermediate disordered phase as the one that we observed in the spin-$\frac{1}{2}$ version of this model between the two quantum triple points at ($\Delta^c = -0.10 \pm 0.15$, $J_2^c/J_1 = 0.505 \pm 0.015$) and ($\Delta^c = 2.05 \pm 0.15$, $J_2^c/J_1 = 0.530 \pm 0.015$), exists for the spin-1 version, for any values of the parameters J_2/J_1 and Δ.

In the context of a spin-wave theory (SWT) treatment of the isotropic J_1–J_2 model on the square lattice, LSWT predicts that quantum fluctuations can destabilize the classical GS with LRO, even at large values of the spin quantum number s, for values of the frustration parameter J_2/J_1 around 0.5. For the spin-$\frac{1}{2}$ case the range of values, $\alpha^{c_1} < J_2/J_1 < \alpha^{c_2}$, for which a magnetically-disordered phase thereby occurs is predicted by LSWT to be given by $\alpha^{c_1} \approx 0.38$ and $\alpha^{c_2} \approx 0.52$. These values may be compared to our own predictions [1] of $\alpha^{c_1} = 0.44 \pm 0.01$ and $\alpha^{c_2} = 0.59 \pm 0.01$. For the spin-1 case LSWT predicts a narrower, but still non-vanishing, strip of disordered intermediate phase in a range with $\alpha^{c_1} \approx 0.47$ and $\alpha^{c_2} \approx 0.501$, whereas we predict with confidence that the disordered phase simply does not exist as a GS in this case.

The discrepancy between our results and those of LSWT for the spin-1 case are undoubtedly due to the shortcomings of LSWT. Thus, while LSWT can work reasonably well in the absence of frustration (e.g., for the isotropic J_1–J_2 model here when $J_2 = 0$, that represents the Heisenberg model with only NN interactions), in the presence of frustration it consistently overestimates the effects of quantum fluctuations. This effect worsens as the frustration (here measured by the ratio J_2/J_1) increases.

Thus, Igarashi [73] has shown explicitly for the J_1–J_2 model by going to higher orders in SWT (i.e., by calculating higher-order terms in the $1/s$ power expansion), that while the series seems to converge for values $J_2/J_1 \lesssim 0.35$, the second-order corrections grow so large for values $J_2/J_1 \gtrsim 0.4$ that no prediction based on LSWT, or even on higher-order SWT, in this region (e.g., about the appearance of an intermediate magnetically-disordered phase near $J_2/J_1 \approx 0.5$) should be relied upon. Furthermore, he showed that the effects of the higher-order correction terms to LSWT make the Néel-ordered state more stable than predicted by LSWT.

Relatively little attention has been paid by other authors to the (pure, isotropic) J_1–J_2 model at higher values of the spin quantum number, $s > \frac{1}{2}$. We note, however, that Cai *et al* [74] have also recently postulated the possible existence of an intermediate phase between the quasiclassical Néel-ordered and collinear stripe-ordered phases for the spin-1 model. More specifically, they hypothesize an intermediate valence-bond solid (VBS) ground state (GS) for the spin-1 isotropic J_1–J_2 model at or near the point of maximal classical frustration where $J_2/J_1 = 0.5$. Their evidence is indirect and is based on a trial variational state of VBS type, which is an *exact* GS of a related spin-1 model Hamiltonian, and on a pseudopotential approach to extend it to the actual spin-1 J_1–J_2 model. They express the dual hopes that this trial state might capture the main character of the disordered phase that they thereby predict for the fully frustrated case, and that accurate numerical methods, such as those considered here, might verify the existence of this postulated intermediate phase. Such variational analyses, based on physically motivated trial states, are always of interest, but have a very chequered history of success in the field of highly correlated spin– and electron–lattice systems. In the present case we stress again that our own detailed numerical analysis provides no evidence at all for the existence of such an intermediate magnetically-disordered VBS phase as postulated by Cai *et al* [74].

In the same context, we note too that in earlier work Read and Sachdev [75] have applied a large-N expansion technique based on symplectic Sp(N) symmetry to the isotropic J_1–J_2 model. They found that the method, which can itself be regarded as akin to a $1/s$ expansion, predicts an intermediate phase (with VBS order) for smaller values of s, but that this phase disappears for larger values of s where they predict instead a first-order transition between the Néel and stripe phases. All of these qualitative results for the pure J_1–J_2 model are in accord with our quantitative predictions.

We note that the results presented here for the spin-anisotropic spin-1 J_1^{XXZ}–J_2^{XXZ} model are also fully consistent with our own previous results [53] for the spatially-anisotropic

spin-1 J_1–J_1'–J_2 model discussed in section 1 above, for which we also found no evidence for an intermediate disordered phase between the quasiclassical Néel and collinear stripe phases with LRO. However, whereas for the spin-1 J_1–J_1'–J_2 model we found strong evidence for a quantum tricritical point at ($J_1'/J_1 \approx 0.66$, $J_2/J_1 \approx 0.35$) where a line of second-order phase transitions between the Néel-ordered and the collinear stripe-ordered states (for $J_1'/J_1 \lesssim 0.66$) meets a line of first-ordered phase transitions between the same two states (for $J_1'/J_1 \gtrsim 0.66$), we find for the present spin-1 J_1^{XXZ}–J_2^{XXZ} model that the phase transition between these two states is first order for all values $\Delta \geqslant 0$. Clearly, these two sets of results are in complete agreement with one another at their common point of overlap, when $J_1' = J_1$ and $\Delta = 1$.

At the XY isotropic point ($\Delta = 0$) of the present spin-1 J_1^{XXZ}–J_2^{XXZ} model we predict that the phase boundary occurs at a value $J_2^c(0) = 0.50 \pm 0.01$. It is interesting to note that our previous results for the spin-$\frac{1}{2}$ version of the model [1] showed a quantum triple point (QTP) at ($\Delta^c = -0.10 \pm 0.015$, $J_2^c = 0.505 \pm 0.015$). Clearly our results for this spin-$\frac{1}{2}$ case are consistent with this lower QTP occurring exactly at the XY isotropic point ($\Delta = 0$) and also at the point of maximum classical frustration, $J_2 = \frac{1}{2}$. Similarly, in the present spin-1 case our results are consistent with the phase boundary at the XY isotropic point also occurring at the point $J_2 = \frac{1}{2}$. It would seem likely, therefore, that for both the cases of spin-$\frac{1}{2}$ and spin-1 particles the corresponding quantum J_1^{XX}–J_2^{XX} model has a special behaviour at the point $J_2/J_1 = \frac{1}{2}$ where the classical frustration is greatest. Our results indicate that a more detailed investigation of this case might, therefore, be worth undertaking for general values of the spin quantum number s.

Although there is very little other accurate numerical work for the present model against which to make comparisons, there have been several previous detailed comparisons, for example, of CCM results with those from the exact diagonalization (ED) of finite spin–lattices for some particular models. One such example [65] is the spin-$\frac{1}{2}$ J–J' (or zigzag) model on the square lattice which contains two kinds of NN isotropic Heisenberg interactions, of strength J and J' respectively, such that each square plaquette contains three J-bonds and one J'-bond, with the J'-bonds arranged in a regular zigzag fashion such that every lattice site on the square lattice is joined to only one J'-bond. An alternative but equivalent description of the model is that it interpolates between a honeycomb and a square lattice, such that the J-bonds join NN lattice sites on the honeycomb lattice, and the J'-bonds join sites across only one of the main diagonals of each hexagon, such that when $J = J'$ the model is equivalent to the NN isotropic Heisenberg model on the square lattice.

ED calculations were performed for the above model [65] for lattices with up to $N = 32$ sites. In general terms it was found that the CCM results for the model at attainable levels of implementation (namely, using the LSUBn approximation with $n \leqslant 8$ agree well with the extrapolated ($N \to \infty$) ED data. The CCM is particularly good, however, at describing both the dimerized and the helical gs phases that this system can support. For the latter phase the ED results lie appreciably above those from the CCM. This is because the energies for the small lattices able to be considered do not fit well to the known theoretical finite-size scaling law in this regime. It is no surprise that finite-size effects for systems with an incommensurate helical spin structure are larger than for systems with Néel order or that are ordered with dimerized spin pairs.

Similar conclusions were also drawn for comparisons of CCM and ED results for extensions of the above spin-$\frac{1}{2}$ J–J' model to both (a) the anisotropic J_{XXZ}–J'_{XXZ} model [57] where both bonds contain an Ising anisotropy of precisely the sort considered in the present paper; and (b) the case where the spin quantum number $s > \frac{1}{2}$ [68]. For the latter case of the spin-1 J–J' model, calculations were performed using both the CCM in the SUBn–n scheme with $n \leqslant 6$ and the ED technique on lattices of sizes $N \leqslant 20$. Again, the resulting finite-size ED extrapolations remained quite poor, and only allowed some qualitative conclusions to be drawn, whereas results from the CCM were seen to be much more robust and more reliable. In no case, however, did the CCM and ED results conflict with each other.

Another model where ED and CCM results have been compared is the pure (isotropic) spin-$\frac{1}{2}$ J_1–J_2 model on the square lattice [76]. Again, the ED results (with $N \leqslant 32$) were found to provide a good qualitative check of the CCM data for LSUBn calculations performed with $n \leqslant 8$. Finally, for the spin-$\frac{1}{2}$ version of the present anisotropic J_1^{XXZ}–J_2^{XXZ} model, we [77] have also compared the CCM results with those from ED calculations on finite-sized lattices of size $N = 36 = 6 \times 6$ sites (with periodic boundary conditions imposed). In this case too the ED data are best used to complement the CCM results. On the basis of all the above evidence we expect that the same will hold true for the spin-1 version of the model studied here. Since the number of basis states increases roughly as 3^N for the spin-1 case, by comparison with 2^N for the spin-$\frac{1}{2}$ case, ED calculations for the present model would be limited to lattices of sizes $N = 16$ and 20. The next biggest lattice that preserves the full lattice symmetry has $N = 26$ sites in this case, and an ED calculation of this size for the spin-1 model is probably beyond the limits of presently available computing power. With only such limited data the ED finite-size extrapolation would again be bound to remain poor, as seen in the previous work cited above, and we fully expect that the CCM results would again prevail even if ED results were available for the present model.

Finally, we note that our analysis and conclusions have relied heavily on two of the unique strengths of the CCM, namely its ability to deal with highly frustrated systems as easily as unfrustrated ones, and its use from the outset of infinite lattices. These, in turn, lead to its ability to yield accurate predictions for the locations of phase boundaries. Our own results for the gs energy and staggered magnetization provide a set of independent checks that lead us to believe that we now have a self-consistent and coherent description of these challenging anisotropic and frustrated J_1^{XXZ}–J_2^{XXZ} systems for both the spin-$\frac{1}{2}$ and spin-1 cases.

Acknowledgments

We thank the University of Minnesota Supercomputing Institute for Digital Simulation and Advanced Computation

for the grant of supercomputing facilities in conducting this research. Two of us (RD and JR) are grateful to the DFG for support (through project Ri615/16-1). We also thank Zi Cai [74], Zhong-Yi Lu [38], Subir Sachdev [75] and Qimiao Si [39] for bringing their respectively cited papers to our attention.

References

[1] Bishop R F, Li P H Y, Darradi R, Schulenburg J and Richter J 2008 *Phys. Rev.* B **78** 054412
[2] Bishop R F 1991 *Theor. Chim. Acta* **80** 95
[3] Bishop R F 1998 *Microscopic Quantum Many-Body Theories and Their Applications* (*Springer Lecture Notes in Physics* vol 510) ed J Navarro and A Polls (Berlin: Springer) p 1
[4] Farnell D J J and Bishop R F 2004 *Quantum Magnetism* (*Springer Lecture Notes in Physics* vol 645) ed U Schollwöck, J Richter, D J J Farnell and R F Bishop (Berlin: Springer) p 307
[5] Haldane F D M 1983 *Phys. Lett.* A **93** 464
Haldane F D M 1983 *Phys. Rev. Lett.* **50** 1153
[6] Chandra P and Doucot B 1988 *Phys. Rev.* B **38** 9335
[7] Ioffe L B and Larkin A I 1988 *Int. J. Mod. Phys.* B **2** 203
[8] Chandra P, Coleman P and Larkin A I 1990 *Phys. Rev. Lett.* **64** 88
[9] Schulz H J and Ziman T A L 1992 *Europhys. Lett.* **18** 355
Schulz H J, Ziman T A L and Poilblanc D 1996 *J. Physique* I **6** 675
[10] Richter J 1993 *Phys. Rev.* B **47** 5794
Richter J, Ivanov N B and Retzlaff K 1994 *Europhys. Lett.* **25** 545
[11] Ivanov N B and Richter J 1994 *J. Phys.: Condens. Matter* **6** 3785
[12] Bishop R F, Farnell D J J and Parkinson J B 1998 *Phys. Rev.* B **58** 6394
[13] Becca F and Mila F 2002 *Phys. Rev. Lett.* **89** 037204
[14] Rosner H, Singh R R P, Zheng W H, Oitmaa J and Pickett W E 2003 *Phys. Rev.* B **67** 014416
[15] Singh R R P, Zheng W, Oitmaa J, Sushkov O P and Hamer C J 2003 *Phys. Rev. Lett.* **91** 017201
[16] Zheng G-M, Hu H and Yu L 2003 *Phys. Rev. Lett.* **91** 067201
[17] Capriotti L, Fubini A, Roscilde T and Tognetti V 2004 *Phys. Rev. Lett.* **92** 157202
[18] Weber C, Becca F and Mila F 2005 *Phys. Rev.* B **72** 024449
[19] Spanu L and Parola A 2005 *Phys. Rev.* B **72** 174418
[20] Sirker J, Weihong Z, Sushkov O P and Oitmaa J 2006 *Phys. Rev.* B **73** 184420
[21] Melzi R, Carretta P, Lascialfari A, Mambrini M, Troyer M, Millet P and Mila F 2000 *Phys. Rev. Lett.* **85** 1318
[22] Melzi R, Aldrovandi S, Tedoldi F, Carretta P, Millet P and Mila F 2001 *Phys. Rev.* B **64** 024409
[23] Carretta P, Papinutto N, Azzoni C B, Mozzati M C, Pavarini E, Gonthier S and Millet P 2002 *Phys. Rev.* B **66** 094420
[24] Kaul E E, Rosner H, Shannon N, Shpanchenko R V and Geibel C 2004 *J. Magn. Magn. Mater.* **272–276** 922
[25] Anderson P W 1987 *Science* **235** 1196
[26] Anderson P W, Baskaran G, Zou Z and Hsu T 1987 *Phys. Rev. Lett.* **58** 2790
[27] Baskaran G and Anderson P W 1988 *Phys. Rev.* B **37** 580
[28] Steiner M, Kakurai K, Kjems J K, Petitgrand D and Pynn R 1987 *J. Appl. Phys.* **61** 3953
[29] Dorner B, Visser D, Steigenberger U, Kakurai K and Steiner M 1988 *Z. Phys.* B **72** 487
[30] Renard J P, Verdaguer M, Regnault L P, Erkelens W A C and Rossat-Mignod J 1988 *J. Appl. Phys.* **63** 3538
[31] Orendáč M, Orendáčová A, Černák J, Feher A, Signore P J C, Meisel M W, Merah S and Verdaguer M 1995 *Phys. Rev.* B **52** 3435
[32] Birgeneau R J, Skalyo J Jr and Shirane G 1970 *J. Appl. Phys.* **41** 1303
[33] Nakatsuji S, Nambu Y, Tonomura H, Sakai O, Jonas S, Broholm C, Tsunetsuga H, Qiu Y M and Maeno Y 2005 *Science* **309** 1697
[34] Tsunetsugu H and Arikawa M 2006 *J. Phys. Soc. Japan* **75** 083701
[35] Bhattacharjee S, Shenoy V B and Senthil T 2006 *Phys. Rev.* B **74** 092406
[36] Chandra P and Coleman P 1991 *Phys. Rev. Lett.* **66** 100
[37] Kamihara Y, Watanabe T, Hirano M and Hosono H 2008 *J. Am. Chem. Soc.* **130** 3296
[38] Ma F, Lu Z-Y and Xiang T 2008 arXiv:0804.3370v3 [cond-mat.mtrl-sci]
[39] Si Q and Abrahams E 2008 arXiv:0804.2480v2 [cond-mat.supr-con]
[40] Schollwöck U, Richter J, Farnell D J J and Bishop R F (ed) 2004 *Quantum Magnetism* (*Springer Lecture Notes in Physics* vol 645) (Berlin: Springer)
[41] Manousakis E 1991 *Rev. Mod. Phys.* **63** 1
[42] Richter J, Schulenburg J and Hoecker A 2004 *Quantum Magnetism* (*Springer Lecture Notes in Physics* vol 645) ed U Schollwöck, J Richter, D J J Farnell and R F Bishop (Berlin: Springer) p 85
[43] Sachdev S 2004 *Quantum Magnetism* (*Springer Lecture Notes in Physics* vol 645) ed U Schollwöck, J Richter, D J J Farnell and R F Bishop (Berlin: Springer) p 381
[44] Misguich G and Lhuillier C 2005 in *Frustrated Spin Systems* ed H T Diep (Singapore: World Scientific) p 229
[45] Villain J 1977 *J. Physique* **38** 385
Villain J, Bidaux R, Carton J P and Conte R 1980 *J. Physique* **41** 1263
[46] Shender E 1982 *Sov. Phys.—JETP* **56** 178
[47] Farnell D J J, Gernoth K A and Bishop R F 2001 *Phys. Rev.* B **64** 172409
[48] Nersesyan A A and Tsvelik A M 2003 *Phys. Rev.* B **67** 024422
[49] Sindzingre P 2004 *Phys. Rev.* B **69** 094418
[50] Starykh O A and Balents L 2004 *Phys. Rev. Lett.* **93** 127202
[51] Moukouri S 2006 *J. Stat. Mech.* P02002
[52] Bishop R F, Li P H Y, Darradi R and Richter J 2008 *J. Phys.: Condens. Matter* **20** 255251
[53] Bishop R F, Li P H Y, Darradi R and Richter J 2008 *Europhys. Lett.* **83** 47004
[54] Benyoussef A, Boubekri A and Ez-Zahraouy H 1998 *Phys. Lett.* A **238** 398
[55] Roscilde T, Feiguin A, Chernyshev A L, Liu S and Haas S 2004 *Phys. Rev. Lett.* **93** 017203
[56] Viana J R and de Sousa J R 2007 *Phys. Rev.* B **75** 052403
[57] Darradi R, Richter J and Krüger S E 2004 *J. Phys.: Condens. Matter* **16** 2681
[58] Roger M and Hetherington J H 1990 *Phys. Rev.* B **41** 200
Roger M and Hetherington J H 1990 *Europhys. Lett.* **11** 255
[59] Bishop R F, Parkinson J B and Xian Y 1991 *Phys. Rev.* B **44** 9425
Bishop R F, Parkinson J B and Xian Y 1992 *Phys. Rev.* B **46** 880
[60] Bishop R F, Hale R G and Xian Y 1994 *Phys. Rev. Lett.* **73** 3157
[61] Xian Y 1994 *J. Phys.: Condens. Matter* **6** 5965
[62] Bursill R, Gehring G A, Farnell D J J, Parkinson J B, Xiang T and Zeng C 1995 *J. Phys.: Condens. Matter* **7** 8605
[63] Zeng C, Farnell D J J and Bishop R F 1998 *J. Stat. Phys.* **90** 327
[64] Rosenfeld J, Ligterink N E and Bishop R F 1999 *Phys. Rev.* B **60** 4030
[65] Krüger S E, Richter J, Schulenburg J, Farnell D J J and Bishop R F 2000 *Phys. Rev.* B **61** 14607
[66] Farnell D J J, Bishop R F and Gernoth K A 2002 *J. Stat. Phys.* **108** 401

[67] Ivanov N B, Richter J and Farnell D J J 2002 *Phys. Rev.* B **66** 014421
[68] Darradi R, Richter J and Farnell D J J 2005 *J. Phys.: Condens. Matter* **17** 341
[69] Schmalfuß D, Darradi R, Richter J, Schulenburg J and Ihle D 2006 *Phys. Rev. Lett.* **97** 157201
[70] Richter J, Darradi R, Zinke R and Bishop R F 2007 *Int. J. Mod. Phys.* B **21** 2273
[71] Zinke R, Schulenburg J and Richter J 2008 *Eur. Phys. J.* B **61** 147
[72] We use the program package 'Crystallographic Coupled Cluster Method' (CCCM) of Farnell D J J and Schulenburg J (see http://www-e.uni-magdeburg.de/jschulen/ccm/index.html)
[73] Igarashi J 1993 *J. Phys. Soc. Japan* **62** 4449
[74] Cai S, Chen S, Kou S and Wang Y 2007 *Phys. Rev.* B **76** 054443
[75] Read N and Sachdev S 1991 *Phys. Rev. Lett.* **66** 1773
[76] Darradi R, Derzhko O, Zinke R, Schulenburg J, Krüger S E and Richter J 2008 arXiv:0806.3825v1 [cond-mat.str-el]
[77] Darradi R, Richter J, Schulenburg J, Bishop R F and Li P H Y 2008 arXiv:0808.2743v1 [cond-mat.str-el]